Dossier

This paper is a part of the hereunder thematic dossier published in OGST Journal, Vol. 70, No. 1, pp. 3-211 and available online here

Cet article fait partie du dossier thématique ci-dessous publié dans la revue OGST, Vol. 70, n°1, pp. 3-211 et téléchargeable ici

DOSSIER Edited by/Sous la direction de : **B. Leduc et P. Tona**

IFP Energies nouvelles International Conference / Les Rencontres Scientifiques d'IFP Energies nouvelles
E-COSM'12 — IFAC Workshop on Engine and Powertrain Control, Simulation and Modeling
E-COSM'12 — Séminaire de l'IFAC sur le contrôle, la simulation et la modélisation des moteurs et groupes moto-propulseurs

Oil & Gas Science and Technology – Rev. IFP Energies nouvelles, Vol. 70 (2015), No. 1, pp. 3-211

IFP Energies nouvelles

Oil & Gas Science and Technology – Rev. IFP Energies nouvelles, Vol. 70 (2015), No. 1, pp. 91-109

DOI: 10.2516/ogst/2013212

OPEN ACCESS

IFP Energies nouvelles International Conference
Rencontres Scientifiques d'IFP Energies nouvelles

E-COSM'12 - IFAC Workshop on Engine and Powertrain Control, Simulation and Modeling
E-COSM'12 - Séminaire de l'IFAC sur le contrôle, la simulation et la modélisation des moteurs et groupes moto-propulseurs

Combustion Noise and Pollutants Prediction for Injection Pattern and Exhaust Gas Recirculation Tuning in an Automotive Common-Rail Diesel Engine

Ivan Arsie[1]*, Rocco Di Leo[1], Cesare Pianese[1] and Matteo De Cesare[2]

[1] *Dept. of Industrial Engineering, University of Salerno, Fisciano (SA) 84084 - Italy*
[2] *Magneti Marelli Powertrain, Bologna 40134 - Italy*
e-mail: iarsie@unisa.it - rodileo@unisa.it - pianese@unisa.it - matteo.decesare@magnetimarelli.com

* Corresponding author

Abstract — *In the last years, emissions standards for internal combustion engines are becoming more and more restrictive, particularly for NO_x and soot emissions from Diesel engines. In order to comply with these requirements, Original Equipment Manufacturers (OEM) have to face with innovative combustion concepts and/or sophisticate after-treatment devices. In both cases, the role of the Engine Management System (EMS) is increasingly essential, following the large number of actuators and sensors introduced and the need to meet customer expectations on performance and comfort. On the other hand, the large number of control variables to be tuned imposes a massive recourse to the experimental testing which is poorly sustainable in terms of time and money. In order to reduce the experimental effort and the time to market, the application of simulation models for EMS calibration has become fundamental. Predictive models, validated against a limited amount of experimental data, allow performing detailed analysis on the influence of engine control variables on pollutants, comfort and performance.*

In this paper, a simulation analysis on the impact of injection pattern and Exhaust Gas Recirculation (EGR) rate on fuel consumption, combustion noise, NO and soot emissions is presented for an automotive Common-Rail Diesel engine. Simulations are accomplished by means of a quasi-dimensional multi-zone model of in-cylinder processes. Furthermore a methodology for in-cylinder pressure processing is presented to estimate combustion noise contribution to radiated noise.

*Model validation is carried out by comparing simulated in-cylinder pressure traces and exhaust emissions with experimental data measured at the test bench in steady-state conditions. Effects of control variables on engine performance, noise and pollutants are analyzed by imposing significant deviation of EGR rate and injection pattern (*i.e. *rail pressure, start-of-injection, number of injections). The results evidence that quasi-dimensional in-cylinder models can be effective in supporting the engine control design toward the optimal tuning of EMS with significant saving of time and money.*

Résumé — **Prédiction du bruit de combustion et des polluants pour le réglage des paramètres d'injection et de l'EGR (*Exhaust Gas Recirculation*) dans un moteur Diesel *Common-Rail* pour l'automobile** — Ces dernières années, les normes d'émissions pour les moteurs à combustion interne sont de plus en plus restrictives, en particulier pour les émissions des NO_x et la production de suie par les moteurs Diesel. Afin de se conformer à ces exigences, les équipementiers (OEM, *Original Equipment Manufacturer*) doivent faire face à des concepts

innovants de combustion et/ou à des dispositifs de post-traitement sophistiqués. Dans les deux cas, le rôle du système de gestion du moteur (EMS, *Engine Management System*) est de plus en plus essentiel, considérant le grand nombre de capteurs et d'actionneurs introduits et l'exigence pour répondre aux attentes de performance et de confort des clients. Par ailleurs, le grand nombre de variables de contrôle à optimiser, impose un recours massif à l'essai expérimental qui est peu rentable pour le rapport temps/argent. Afin de réduire l'effort expérimental et le délai de mise sur le marché, l'application des modèles de simulation pour le calibrage de l'EMS est fondamentale. Les modèles prédictifs, validés par rapport à un nombre limité de données expérimentales, permettent de réaliser des analyses détaillées sur l'influence des variables de contrôle du moteur sur les polluants, le confort et les performances. Cet article présente une analyse de simulation sur l'impact des paramètres d'injection et du taux de recirculation des gaz d'échappement (EGR, *Exhaust Gas Recirculation*) sur la consommation de carburant, le bruit de combustion, les émissions de NO et la production de suie par le moteur automobile Diesel *Common-Rail*. Les simulations sont effectuées par un modèle multi-zone, quasi-dimensionnel des phénomènes internes au cylindre. Cet article présente également une méthode pour le traitement de la pression interne au cylindre afin d'évaluer le bruit de combustion par rapport au bruit émis. La validation du modèle est effectuée en comparant la pression interne au cylindre et les émissions d'échappement simulées aux données expérimentales traitées au banc d'essai en régime stationnaire. Les effets des variables de contrôle sur les performances du moteur, le bruit et les polluants sont analysés en imposant la variation du taux de l'EGR et les paramètres d'injection (par exemple la pression du rail, le début d'injection et le nombre d'injections). Les résultats démontrent que les modèles quasi-dimensionnels des phénomènes internes au cylindre peuvent être efficaces à la conception du contrôle du moteur pour optimiser le réglage de l'EMS avec un gain de temps et d'argent.

NOMENCLATURE

b_i	Injection calibration parameter (-)
$BMEP$	Break Mean Effective Pressure (bar)
C_1	Calibration factor for spray impingement (-)
C_2	Parameter of the turbulence model (-)
C_3	Empirical parameter for ignition delay (-)
C_4	Proportional factor of eddy turnover (-)
E	Activation energy (J/mol)
EID	Effective Injection Duration (ms)
ET	Energizing Time (ms)
E_{ith_zone}	Internal energy in the *i*-th zone (J)
h_{ith_zone}	Specific enthalpy in the *i*-th-zone (J/kg)
$IMEP$	Indicated Mean Effective Pressure (bar)
ISD	Injection Start Delay (ms)
L	Current number of radial parcels (-)
L_I	Integral length scale (m)
L_h	Maximum number of radial parcels (-)
m_{ae}	Mass of entrained air (kg)
m_b	Mass of burned fuel (kg)
m_e	Mass of evaporated fuel (kg)
$m_{f,inj}$	Mass of injected fuel (kg)
m_{ith_zone}	Fuel mass in the *i*-th zone (kg)
m_v	Mass of fuel vapor (kg)
N_{rad}	Maximum number of radial parcels (-)
n_{fv}	Molar fraction of fuel vapor (-)
n_{O_2}	Molar fraction of oxygen (-)
$PCCI$	Premixed Combustion Compression Ignition
p_{rail}	Common rail pressure (bar)
p	In-cylinder pressure (bar)
p_{eff}	Sound pressure (Pa)
p_0	Pressure hearing threshold (Pa)
Q_{ith_zone}	Heat transfer rate to the *i*-th zone (J)
R_0	Universal gas constant (J/(mol.K))
S	Penetration of the generic spray core parcel (m)
S_L	Radial penetration of the *L*-th parcel of spray (m)
SOI	Start Of Injection (°ATDC)
SOC	Start Of Combustion (°ATDC)
T	In-cylinder temperature (K)
T_b	Temperature of burned gas (K)
T_{eff}	Time period for sound pressure evaluation (s)
u'	Turbulence intensity (m/s)
U_f	Initial spray velocity (m/s)
U_{mp}	Mean piston velocity (m/s)
V_a	Air-zone volume (m^3)

V_{cyl} Instantaneous cylinder volume (m^3)
V_{finj} Volume of injected fuel (m^3)
V_{ith_zone} Instantaneous volume of the *i*-th zone (m^3)
W_{ith_zone} Work transfer rate out of the *i*-th zone (J)

Greek Symbols

γ Weight factor (-)
ρ Air zone density (kg/m^3)
τ_b Characteristic combustion time (s)
$\tau_{b,lam}$ Characteristic time of laminar combustion (s)
$\tau_{b,turb}$ Characteristic time of turbulent combustion (s)
τ_{id} Ignition delay (s)

INTRODUCTION

The interest in Diesel engines for automotive application has dramatically grown in the last decade, due to the benefits gained with the introduction of common-rail system and electronic control. A strong increase in fuel economy and a remarkable reduction of emissions and combustion noise have been achieved, thanks to both optimized fuelling strategy and advanced fuel injection technology. Namely, the improvement of injector time response, injection pressure and nozzle characteristics have made feasible the operation of multiple injections and have enhanced the fuel atomization. The actuation of early pilot and pre injections enhances the occurrence of a smoother combustion process with benefits on noise. Improved fuel atomization enhances the air entrainment making the combustion cleaner and more efficient, thus reducing both particulate emissions and fuel consumption but with a negative impact on NO_x emissions (Tennison and Reitz, 2001). On the other hand, the recourse to Exhaust Gas Recirculation (EGR) lowers in-cylinder peak temperature and NO_x emissions but with a negative impact on particulate emissions.

In the last years, many efforts are addressed towards new combustion concepts, in order to face with the soot/NO_x trade-off and the increasingly restrictive emission standards. Earlier injections and large EGR rate promote premixed combustion and lead to lower peak temperature, with benefits on both particulate and NO_x emissions. The drawback is the increase of combustion noise, due to the large delay of premixed combustion up to the Top Dead Center (TDC) that results in a dramatic and sharp increase of in-cylinder pressure (Torregrosa *et al.*, 2011). In this context, it is clear that a suitable design of engine control strategies is fundamental in order to overcome with the simultaneous and opposite impact of combustion law on NO_x/soot emissions and combustion noise. Nevertheless the large number of control variables (*i.e.* injection pattern, EGR, Variable Geometry Turbine (VGT) rack position) makes the experimental testing extremely expensive in terms of time and money. Massive use of advanced mathematical models to simulate engine and system components (mechanical and electronic devices) is therefore recommended to speed up the design and optimization of engine control strategies.

The complexity of Diesel engine combustion, which is governed by the turbulent fuel-air-mixing, causes an unresolved trade-off between computational time and accuracy. Single zone models based on empirical heat release laws, largely used to simulate SI engine performance and emissions, are inadequate to simulate the heterogeneous character of Diesel combustion (Barba *et al.*, 2000). This problem is particularly felt for emissions prediction; in that case a huge effort has to be spent for parameters identification to reach a satisfactory accuracy. Therefore, in order to achieve suitable precision, most of the studies in the field of Diesel engine modeling have focused on the basic phenomena involved into fuel injection/evaporation, air entrainment, combustion and emission formation, with particular emphasis on particulate matter (mainly soot). On the other hand, many advanced models are available in the literature, based on the complete 3D description of turbulent, multi-phase flow field inside the cylinder (Gang and Tao, 2010; López *et al.*, 2013; Javadi Rad *et al.*, 2010). Despite their accuracy, these models present a large computational demand and are indeed oriented to engine design (combustion chamber shaping, fuel jet/air interaction, swirl) rather than to control design application.

Phenomenological two-zone or multi-zone combustion models have been proposed in literature to meet the requirements for engine control design. Such models are accurate enough to predict fuel evaporation, air entrainment, fuel-air distribution and thermal stratification with a reasonable computational demand (Kouremenos *et al.*, 1997; Arsie *et al.*, 2006). Particularly, the identification analysis of the main model parameters enhances the development of predictive tools for efficient and accurate simulation of the effects of control injection variables on combustion process and exhaust emissions formation (Rakopoulos *et al.*, 2003; Arsie *et al.*, 2007, 2012).

In the present paper, a multi-zone model is applied to simulate engine combustion and predict noise and pollutant emissions depending on injection pattern and EGR rate. The novelties with respect to previous works presented by the authors (Arsie *et al.*, 2006, 2007, 2012) are the development of improved models for fuel

injection and ignition delay and a methodology to estimate the combustion noise.

1 MULTI-ZONE MODEL

Simulation of in-cylinder pressure is accomplished by a thermodynamic model, which is based on the energy conservation for an open system and on the volume conservation of the total combustion chamber (Assanis and Heywood, 1986; Hiroyasu and Kadota, 1983; Bi *et al.*, 1999; Arsie *et al.*, 2006):

$$\dot{E}_i = \dot{Q}_i - \dot{W}_i + \sum_{j,i\neq j} \dot{m}_{i,j} \times h_{i,j} \quad (1)$$

$$V_{cyl} = V_a + \sum_i V_i \quad (2)$$

The combustion chamber is divided into several zones, with homogeneous pressure and different temperature and chemical composition. In each zone, the gas is assumed ideal and the thermodynamic properties are function of temperature, pressure and composition (Ferguson, 1986). During the compression stroke, only one homogeneous zone containing air and residual gas (air zone, a) is considered as shown in Figure 1.

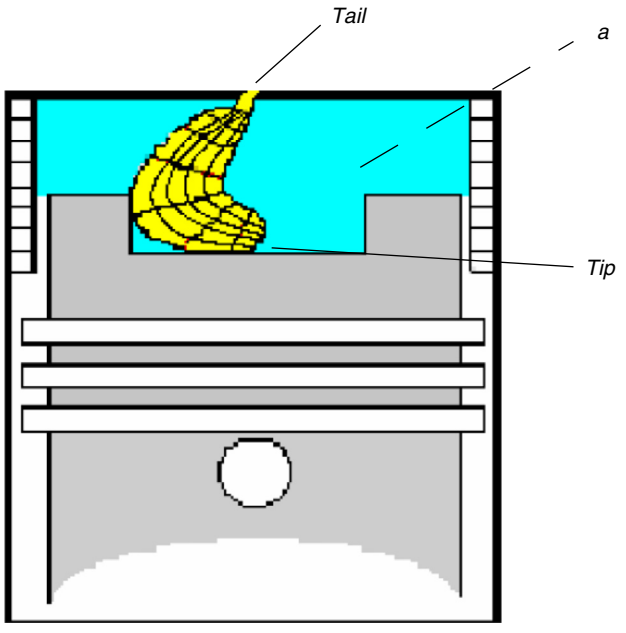

Figure 1

Scheme of in-cylinder stratification with air zone (a) and spray discretization in axial and radial direction.

When the injection takes place, the fuel jet forms a number of sprays, depending on the number of injection nozzle holes. Each spray is divided into several parcels along both axial and radial direction. For each parcel, a burned zone composed by combustion products and an unburned zone composed by fuel, entrained air and residual gas, are considered. This process is repeated for each injection, neglecting interactions among the sprays and energy or mass transfer among the parcels (Arsie *et al.*, 2006). The model simulates temperature and chemical composition in each parcel thus enhancing prediction of NO and soot engine emissions.

1.1 Fuel Injection

Fuel injection strongly affects the heat release rate and its modeling is a critical issue to deal with. This is also due to the lack of experimental data collected at the flow test bench on the injection rate shape which inhibits the development of data-driven models. Nowadays several multi-dimensional commercial codes are available to model mechanical, hydraulic and electromagnetic phenomena, thus taking into account the inertia and the dynamics of every component inside the injector. Nevertheless these approaches involve a huge computational effort, not suitable for the current model application.

In order to overcome this issue, in the model presented herein the injection rate shape is simulated by an empirical formulation derived from a set of experimental data measured at the flow test bench. Figure 2 shows the

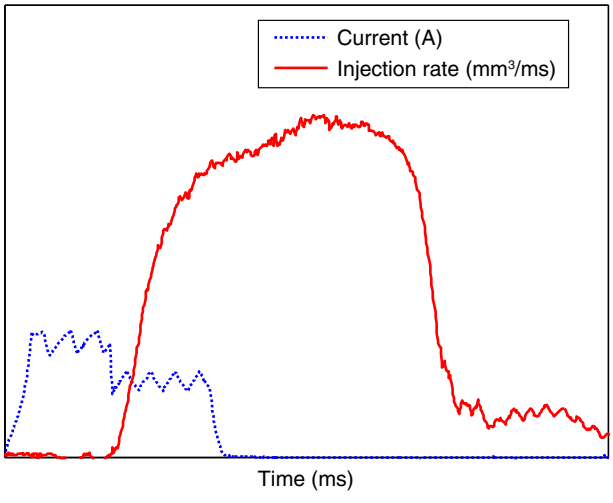

Figure 2

Experimental injection rate shape. P_{rail} = 1 600 bar, ET = 730 µs. The scales are omitted for confidential issues.

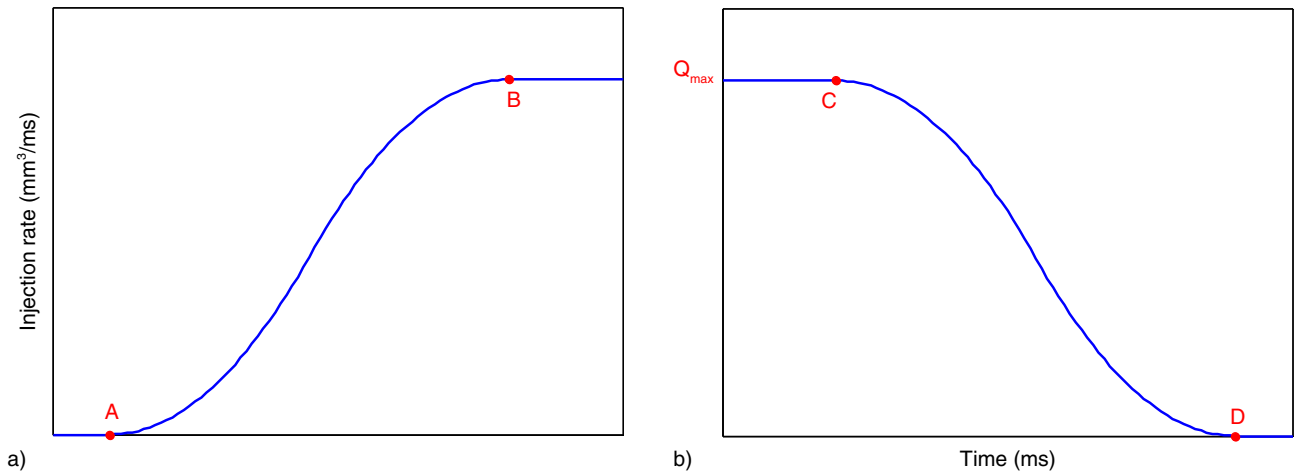

Figure 3

a) *S*- and b) *Z*- functions defined to describe the injection rate trajectory.

injection rate shape experimentally detected for a Common-Rail injector in case of rail pressure (P_{rail}) and Energizing Time (ET) set at 1 600 bar and 730 μs, respectively. Figure 2 evidences that the experimental injection rate trajectory does not correspond to a regular geometrical shape; it usually shows fluctuations around the maximum flow rate, due to the wave effects inside the injector pipes. However, at least for the main injections, such fluctuations can be neglected without significant lack of accuracy. The mentioned maximum flow rate, which depends on common rail and combustion chamber pressure and on the characteristics of the injector, is calculated from the static flow rate provided by the manufacturer. Nevertheless, it is worth noting that in case of short injection timing, the static flow rate might not be reached and the maximum flow rate has to be evaluated differently, as it will be described later.

Following the experimental trajectory, the injection rate shape was modeled by coupling two symmetric curves, namely a *S*-function and a *Z*-function which account for needle lift and closing, respectively, as shown in Figure 3.

The *S*-function can be defined by means of three parameters corresponding to:

- the Injection Start Delay (ISD) (point A in *Fig. 3*);
- the time at which the maximum flow rate is reached (point B);
- the maximum flow rate reached (Q_{max}).

Being symmetric, the *Z*- function was derived consequently. It is worth noting that the ISD is defined as the time it takes from the start of injector Energizing Time (ET) and the effective fuel flowing through the nozzle (Coppo and Dongiovanni, 2007). Moreover, the time range defined by the points A and D in Figure 3 corresponds to the Effective Injection Duration (EID). The three parameters ISD, EID and Q_{max} are expected to be dependent on needle inertia, rail pressure and back-pressure into the combustion chamber (*i.e.* in-cylinder pressure).

The parameters identification was accomplished making use of a set of experimental injector rate trajectories, ranging the ET and P_{rail} as reported in Table 1. Particularly, from the analysis of the experimental data, the ISD resulted to be almost constant and it was set to 0.335 ms for all the operating conditions. On the other hand, the EID was identified for each operating condition and finally expressed as function of rail pressure and ET by the following relationship:

TABLE 1

Values of rail pressure (P_{rail}) and Energizing Time (ET) experimentally investigated for the injection rate identification

Test case	P_{rail} (bar)	ET (μs)
1	740	285
2	740	525
3	800	345
4	800	650
5	1 600	315
6	1 600	750

$$EID = b_1 + b_2 \times P_{rail} + b_3 \times ET \quad (3)$$

with the parameters b_1, b_2 and b_3 equal to -0.574, -1.60×10^{-5} and 2.60×10^{-3}, respectively, for the current injection system.

Finally, the maximum flow rate Q_{max} was identified by recursive processing of S- and Z- functions, in order to achieve the target mass of injected fuel.

The comparison between measured and estimated injection rate trajectories for the six test cases considered is shown in Figure 4, which exhibits a good accuracy of the developed injector rate model.

1.2 Fuel Spray and Evaporation

The injected fuel moves as a liquid column, until the break-up time elapses. Then it is assumed that the fuel atomizes to fine droplets which move into the combustion chamber decreasing their velocity while entraining the surrounding air (Hiroyasu and Masataka, 1990; Jung and Assanis, 2006). The break-up time is calculated using the correlations proposed by Hiroyasu and Kadota (1983). The spatial development of the spray is simulated using the Naber correlation (Naber and Siebers, 1996). This quasi-dimensional approach allows estimating the spray penetration along the central axial direction. The radial discretization is defined generalizing the correlation proposed by Hiroyasu and Kadota (1983), as follows:

$$S_L = S \cdot \exp\left[-8.557 \cdot 10^{-3} \cdot \frac{(L_h - 1)^2}{(N_{rad} - 1)^2} \cdot (L - 1)^2\right] \quad (4)$$

where S is the penetration of the generic spray core parcel, S_L is the penetration of the L-th parcel of spray in radial direction, $L_h = 10$ is the maximum number of radial parcels considered by Hiroyasu and Kadota (1983) and Hiroyasu and Masataka (1990), N_{rad} is the current number of radial parcels.

The air entrainment model is derived from the momentum conservation law:

$$\dot{m}_{ae} = -C_1 \frac{m_{f,inj} \times U_f}{\left(\frac{dS}{dt}\right)^2} \times \frac{d^2S}{dt^2} \quad (5)$$

where the parameter C_1 accounts for the influence of air swirl and the effects of the spray impingement on piston bowl and/or cylinder wall. For the current study, the parameter C_1 was identified by fitting measured and simulated in-cylinder pressure for five engine operating conditions at constant engine speed and increasing load.

After the break-up time, due to the high surrounding gas temperature, the droplets evaporate and mix with the entrained air. For a complete description of the fuel evaporation model the reader is addressed to a previous paper (Arsie *et al.*, 2006). Its approach relies on the equations of the mass diffusion and heat transfer for a spherical droplet with initial diameter equal to the Sauter Mean Diameter (SMD) (Hiroyasu and Kadota, 1983; Kuo, 1986; Jung and Assanis, 2006). Moreover the model assumes the heat transfer to the cylinder wall as sum of radiative and convective heat transfer, following the Woschni formulation (Ramos, 1989). The total heat transfer is shared among the zones according with their mass and temperature.

1.3 Turbulence Model

The turbulence model is based on the k-ε approach. The values of the turbulent kinetic energy (k) and its dissipation rate (ε) have been assumed homogeneous in the combustion chamber and they have been computed by the two following equations (Ramos, 1989):

$$\frac{dk}{dt} = \frac{2}{3}\frac{k}{\rho}\frac{d\rho}{dt} - \varepsilon \quad (6)$$

$$\frac{d\varepsilon}{dt} = \frac{4}{3}\frac{\varepsilon}{\rho}\frac{d\rho}{dt} - \frac{2\varepsilon^2}{k} \quad (7)$$

These equations do not consider the combustion influence on the turbulence.

The initial condition of k at Intake Valve Closing (IVC) is estimated considering its definition for isotropic homogeneous turbulence and assuming that the initial value of the turbulence intensity (u') depends on the mean piston velocity:

$$k = \frac{3}{2}(u\prime)^2 \quad (8)$$

$$k(IVC) = C_2 \frac{3}{2}\left(U_{mp}\right)^2 \quad (9)$$

where $C_2 = 0.10$.

The initial value of ε is estimated assuming the equilibrium between production and dissipation of turbulence kinetic energy (Ramos, 1989):

$$\varepsilon(IVC) = \frac{[k(IVC)]^{3/2}}{L_I(IVC)} \quad (10)$$

where L_I is the integral length scale, whose value at IVC was set to 10 mm, corresponding to the maximum intake

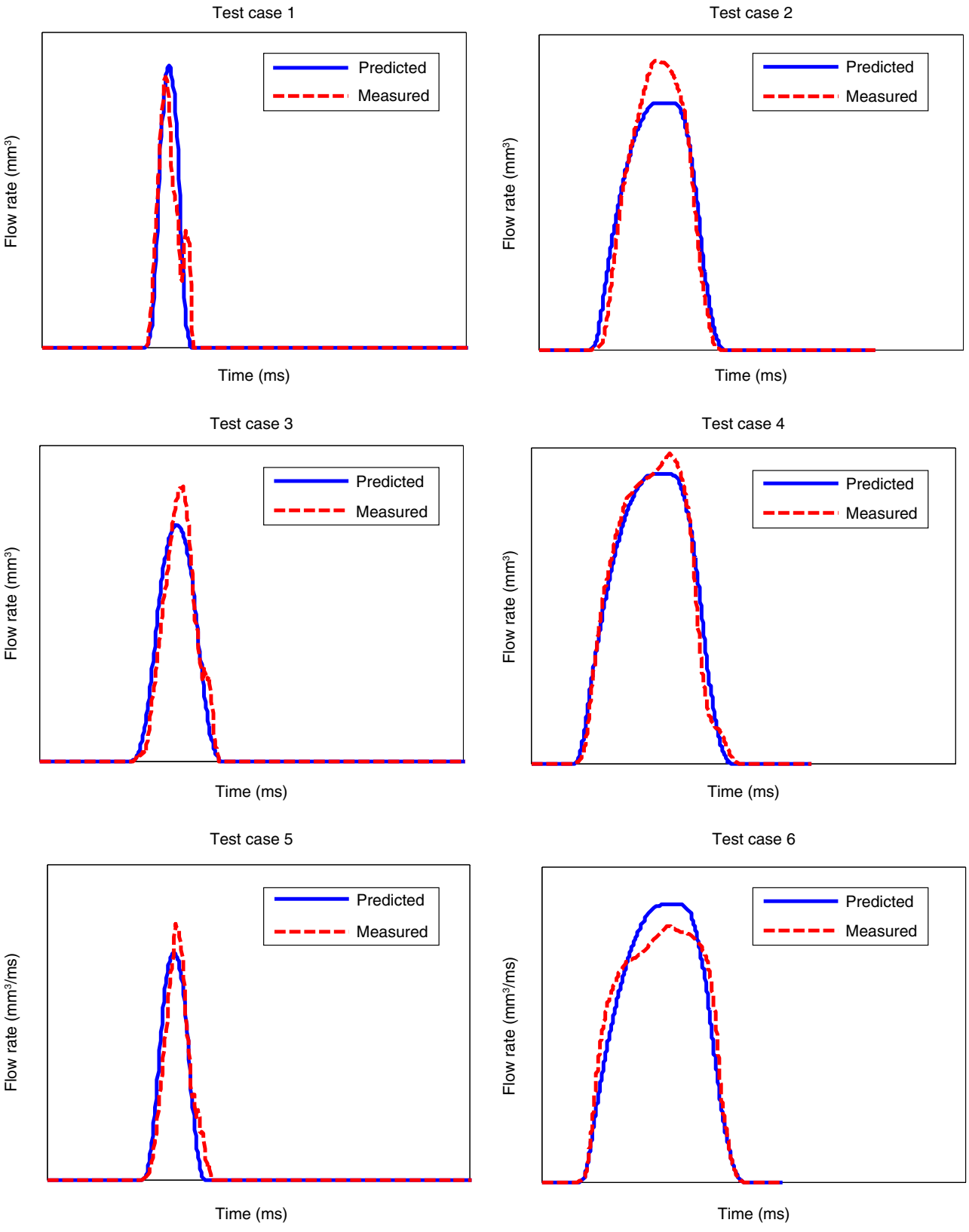

Figure 4

Comparison between measured and predicted injection rate trajectories.

valve lift. At IVC, Equations (9) and (10) are used to calculate u' and L_I to fix the initial condition of Equations (6) and (7).

1.4 Ignition Delay

The ignition delay is due to the combustion kinetics which depends on the cylinder pressure and temperature at the injection timing through an Arrhenius correlation (Hiroyasu and Kadota 1983):

$$\tau_{id} = C_3 p^{-1.02} \phi^{-0.1} \exp\left(\frac{1600}{T}\right) \tag{11}$$

where p and T are the in-cylinder pressure and temperature, respectively, ϕ is the equivalent ratio of the mixture. C_3 is an empirical parameter and was set to 3.45 according with literature data (Heywood, 1988).

1.5 Combustion

The combustion model is based on the laminar and turbulent characteristic-time approach (Kong *et al.*, 1995; Tanner and Reitz, 1999; Ayoub and Reitz, 1995). The fuel combustion in the burning region is described by the following equation (Ramos, 1989):

$$\frac{dm_b}{dt} = \frac{m_e - m_b}{\tau_b} \tag{12}$$

where the characteristic time τ_b is the same for each chemical reactant. In order to account for the effects of turbulence on the chemical reactions, the characteristic time is calculated as the weighted sum of the laminar timescale ($\tau_{b,lam}$) and the turbulent timescale ($\tau_{b,turb}$):

$$\tau_b = \tau_{b,lam} + \gamma \tau_{b,turb} \tag{13}$$

with the weight γ given as:

$$\gamma = \frac{1 - e^{-x}}{0.632} \tag{14}$$

where x is the burned fuel fraction defined as:

$$x = \frac{m_b}{m_v} \tag{15}$$

Zeroing the concentration of fuel at equilibrium, the laminar time scale is computed as:

$$\tau_{b,lam} = \left(7.68 \times 10^8 \left[n_{fv}\right]^{-0.75} \times \left[n_{O_2}\right]^{1.5} \exp\left(-\frac{E}{R_0 T_b}\right)\right)^{-1} \tag{16}$$

where $E = 77.3 \times 10^3$ J/mol and $R_0 = 8.3144$ J/(mol.K).

Finally the turbulent combustion time is function of the eddy turnover:

$$\tau_{b,turb} = C_4 \frac{k}{\varepsilon} \tag{17}$$

the proportional factor C_4 was set to 0.142 according with literature data (Kong *et al.*, 1995; Tanner and Reitz, 1999; Ayoub and Reitz, 1995).

1.6 Nitrogen Oxide Emissions

NO_x emissions from Diesel engines are mainly due to the thermal NO formation for dilute (lean mixture and EGR) operation (Heywood, 1988). The thermal NO formation process is modeled making use of the well-known extended Zeldovich mechanism applied to the mixing zone, which considers three reactions with seven species as main responsible for NO production (Heywood, 1988; Ramos, 1989; Arsie *et al.*, 2006, 2007).

More detailed models have been proposed, as the super extended Zeldovich mechanism by Miller *et al.* (1998), which accounts for 13 species and up to 67 reactions and can led to a significant improvement of model accuracy. On the other hand, this approach could thwart the benefits of phenomenological models because of its higher computational complexity.

According with the well known assumptions on steady state nitrogen formation and equilibrium concentration for the reactants (Heywood, 1988), the Zeldovich mechanism holds the following rate of variation for the NO concentration:

$$\frac{1}{V_b}\frac{dn_{NO}}{dt} = \frac{2R_1\left\{1 - \left(\frac{[NO]}{[NO]_{eq}}\right)^2\right\}}{1 + \left(\frac{[NO]}{[NO]_{eq}}\right)\frac{R_1}{R_2 + R_3}} \tag{18}$$

where n_{NO} is the number of NO moles in the burned gas volume V_b, while R_1, R_2 and R_3 are computed as follows:

$$R_1 = k_1^+ [O]_e [N_2]_e \quad k_1^+ = 7.6 \times 10^{13} \exp\left(\frac{-38\ 000}{T}\right)$$
$$R_2 = k_2^- [NO]_e [O]_e \quad k_2^- = 1.5 \times 10^9 \exp\left(\frac{-19\ 500}{T}\right)$$
$$R_3 = k_3^- [NO]_e [H]_e \quad k_3^- = 2 \times 10^{14} \exp\left(\frac{-23\ 650}{T}\right)$$

The temperature T is in Kelvin, the concentrations are in mol/cm^3 and the subscript e denotes chemical equilibrium.

The indicated reaction rate constants k_1, k_2 and k_3 are the most frequently used in the literature (Heywood, 1988; Ramos, 1989) and they could present some

uncertainty depending on actual temperature and pressure. Several studies have been proposed in order to identify the optimal parameters at different engine operation. Among the others, Miller *et al.* (1998) proposed a correction factor for the constant k_1 as function of the instantaneous in-cylinder pressure; at high engine load and pressure, the reaction rate is reduced up to 80% of the original value, with a significant reduction of the NO prediction. The authors themselves have proposed an identification method based on a decomposition approach for estimating the optimal parameters as function of the engine operating conditions, with a significant improvement of model accuracy on a wide set of reference data (Arsie *et al.*, 1998).

1.7 Soot Emissions

The mechanism of particulate formation is one of the most critical tasks in Diesel engine modeling. The basic phenomena that characterize the formation, the growth and the oxidation of the soot particles are not completely understood yet. The attempts performed for estimating soot emissions have led to the development of a wide variety of models ranging from phenomenological to empirical (black-box).

The most widely adopted modeling approach is the one originally proposed by Hiroyasu, which describes the soot formation and oxidation processes as kinetically controlled by two Arrhenius equations (Hiroyasu and Kadota, 1983). Thus the net soot mass rate is given by the difference between the mass formation rate and the mass oxidation rate (Patterson *et al.*, 1994):

$$\frac{dm_s}{dt} = \frac{dm_{sf}}{dt} - \frac{dm_{so}}{dt} \tag{19}$$

The mass formation rate m_{sf} and the mass oxidation rate m_{so} are estimated as:

$$\frac{dm_{sf}}{dt} = A_f m_{fv} P^{0.5} \exp\left(-E_f/RT\right) \tag{20}$$

$$\frac{dm_{so}}{dt} = A_o m_s Y_{O_2} P^{1.8} \exp\left(-E_o/RT\right) \tag{21}$$

where m_{fv} and m_s are the mass of fuel vapour and the net mass of soot, respectively, P is the in-cylinder pressure, Y_{O_2} is the oxygen molar fraction, T is the temperature. The pre-exponential coefficients A_f and A_o are model parameters to be identified in order to fit the experimental measurements; for the current analysis the identification was performed with respect to one operating point, corresponding to engine operation at medium load with EGR. The activation energies E_f and E_o are assumed equal to 12 500 cal/mol and 14 000 cal/mol, as suggested by Hiroyasu and Kadota (1983).

The model given by Equations (19, 20) and (21) has been widely implemented in the framework of multi-zone combustion models (Patterson *et al.*, 1994); the soot and oxidation kinetic equations are solved independently for each zone, which is characterized by uniform pressure, temperature and chemical composition. The total soot emissions are then estimated considering the contributions of all the zones. A different approach was proposed by Bayer and Foster (2003) who developed a detailed spray model and solved the soot formation and oxidation equations (20) and (21) for the whole region bounded by the fuel diffusion flame. This assumption is based on the hypothesis that the soot formation is mainly due to the fuel pyrolysis in the rich core, which is characterized by uniform temperature and composition.

2 MODEL VALIDATION

The present section is devoted to analyze model accuracy by comparing the simulations against a set of experimental data measured at the test bench. The reference engine is a light-duty, 4 cylinders, EURO 5 Diesel engine, equipped with common-rail injection system, high pressure EGR and Variable Geometry Turbine (VGT), whose main characteristics are described in Table 2.

Model accuracy was evaluated *via* comparison between predicted and measured in-cylinder pressure, NO and soot emissions at 34 different engine operating conditions, with engine speed ranging from 1 000 to 4 500 rpm, BMEP ranging from min to max, EGR rate ranging from 0 to 35%. Furthermore operations with single, double or multiple fuel injections were investigated.

Figure 5-9 show the comparison between predicted and measured in-cylinder pressure traces for five engine

TABLE 2
Engine technical data

Cylinders	4 in line
Displaced volume	1 248 cc
Valves per cylinder	4
Max. power	70 kW @ 4 000 rpm
Max. torque	210 Nm @ 1 750 rpm
Fuel injection system	Common rail solenoid injectors
Compression ratio	16.8:1

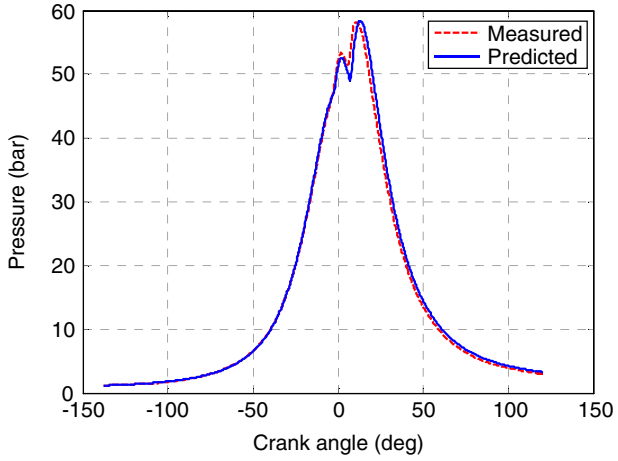

Figure 5

Comparison between measured and predicted in-cylinder pressure. Test case 1.

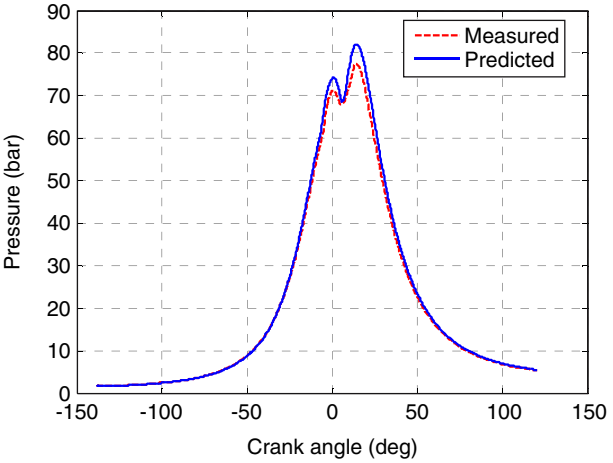

Figure 7

Comparison between measured and predicted in-cylinder pressure. Test case 3.

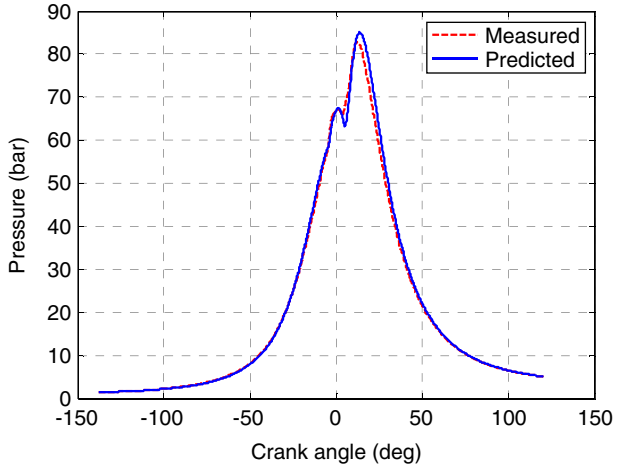

Figure 6

Comparison between measured and predicted in-cylinder pressure. Test case 2.

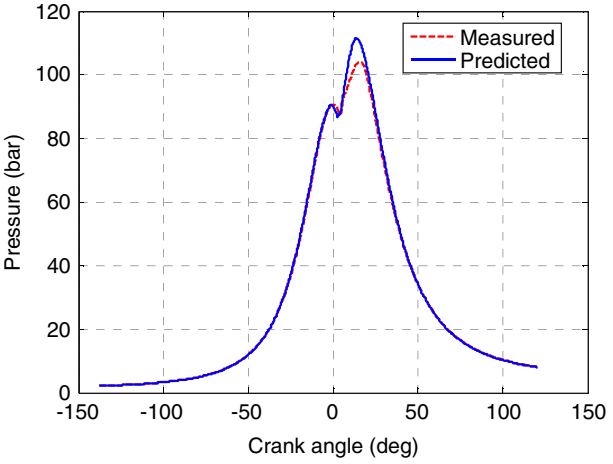

Figure 8

Comparison between measured and predicted in-cylinder pressure. Test case 4.

operating conditions, with different engine speed, load, fuel injections patterns and EGR rate, as reported in Table 3. In all cases, the model exhibits a good accuracy in predicting the engine cycle, even in the most critical conditions in case of high EGR rate (*i.e. Fig. 5, 9*). The model accuracy on the whole data set (34 cases) is shown in Figure 10 where the comparison between measured and predicted gross IMEP is shown. The figure evidences a good agreement with a correlation index R^2 equal to 0.995.

Figures 11-14 show model accuracy in estimating soot and NO emissions, respectively, by a comparison of predicted and measured data. The results refer to ten operating conditions at 2 000 rpm and 2 500 rpm, with increasing BMEP and rail pressure and different EGR rates.

Figures 11 and 12 apparently show poor validation results for the soot model with a quite large error. Nevertheless the model catches the main trends *versus* engine operating conditions, with the initial rise due to load increase and the final reduction due to the strong EGR reduction. An opposite trend is observed as BMEP increases from 4 to 8 bar at 2 000 rpm and EGR is reduced from 30% to 20%. This different

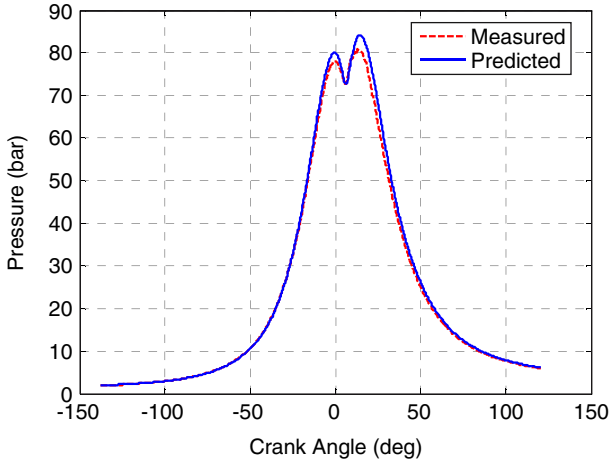

Figure 9

Comparison between measured and predicted in-cylinder pressure. Test case 5.

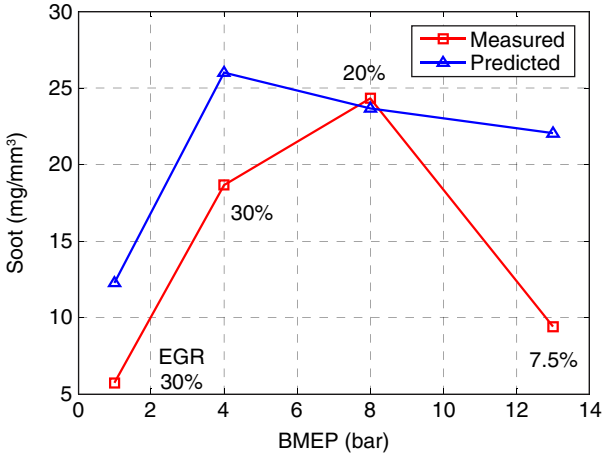

Figure 11

Comparison between measured and predicted engine soot emissions, *versus BMEP* at engine speed = 2 000 rpm. The numerical values in the plot indicate the EGR rate for each operating condition.

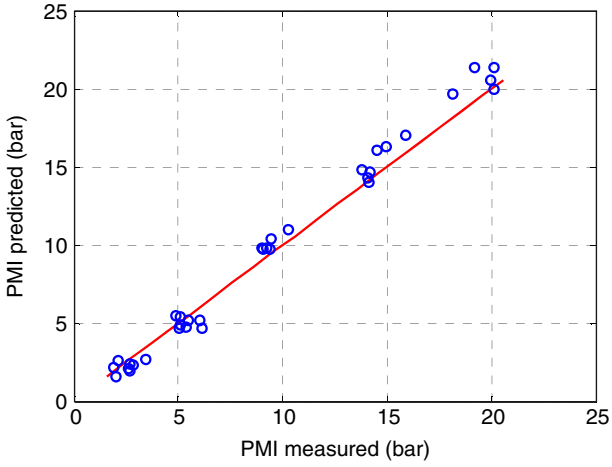

Figure 10

Comparison between measured and predicted IMEP for the whole set of experimental data. $R^2 = 0.99554$.

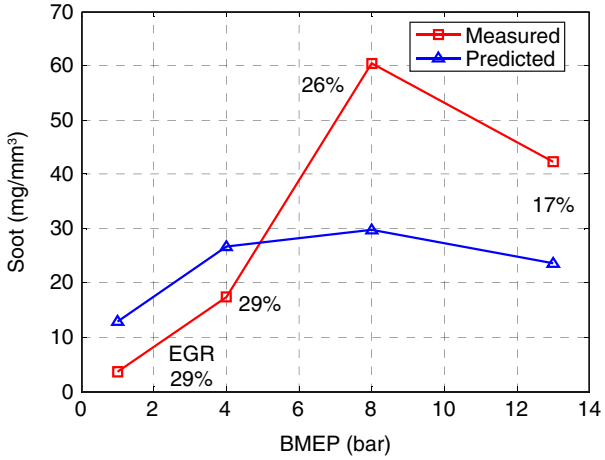

Figure 12

Comparison between measured and predicted engine soot emissions, *versus BMEP* at engine speed = 2 500 rpm. The numerical values in the plot indicate the EGR rate for each operating condition.

TABLE 3

Test cases considered for model validation

Test case	Speed (rpm)	BMEP (bar)	EGR (%)	P_{rail} (bar)	SOI (°ATDC) pil/pre/main
1	1 500	4	32	450	−24/−12/−2.5
2	1 500	8	16	615	−20/−9/−2
3	2 000	8	20	700	−30/−16/−3
4	2 500	13	17	1 000	−29/−7
5	3 000	8	25	910	−23/−6

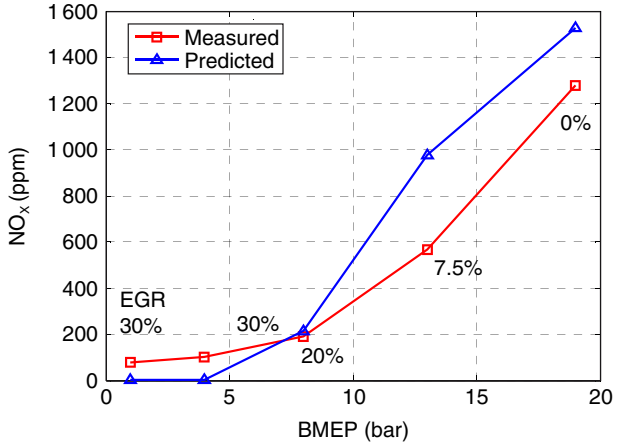

Figure 13

Comparison between measured and predicted engine NO emissions *versus BMEP* at engine speed = 2 000 rpm. The numerical values in the plot indicate the EGR rate for each operating condition.

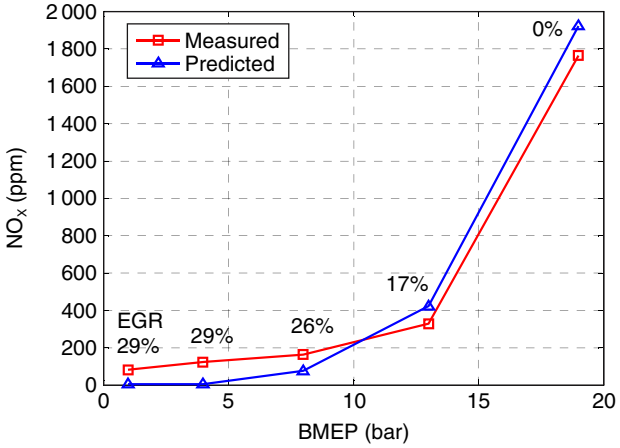

Figure 14

Comparison between measured and predicted engine NO emissions *versus BMEP* at engine speed = 2 500 rpm. The numerical values in the plot indicate the EGR rate for each operating condition.

behaviour may be due the superposition of the following effects:

- overestimation of the increased soot oxidation due to greater in-cylinder temperature;
- underestimation of increased soot formation due to greater mass of fuel. These effects also explain the underestimation detected at 2 500 rpm and BMEP equal to 8 and 13 bar.

It is worth noting that soot measurement is very often affected by large uncertainty due to the poor reliability of the instruments used, which are frequently based on empiric laws. Recently, more sophisticated and reliable instruments are coming up but they were not available for the current analysis. This is one of the motivations why physical models, even more complex that this (Patterson *et al.*, 1994; Hountalas, 2008), rarely exhibit a mean relative error below 50% in the whole engine operating domain. Few simulation results showing higher accuracy focus the analysis on three/four engine operating conditions very close each other (Jung and Assanis, 2006).

Finally, regardless to the entity of the validation error, model worthiness can be assessed by simulating soot emissions with perturbation of injection pattern and EGR and verifying whether the results are in accordance with the trends expected from experimental investigation. This parametric analysis is presented in Section 4.

Figures 13 and 14 evidence the good model results in predicting NO emissions with respect to measurements. The figures show the expected increasing trend of NO with the load, due to the higher in-cylinder temperature following increased injected fuel mass and reduced EGR rate. Poor accuracy is reached at low load, because the Zeldovich mechanism only accounts for thermal NO formation thus lacking accuracy when low in cylinder temperature is reached. Nevertheless it is worth noting that the proposed model is intended to support the EMS tuning in compliance with NO_x/soot regulations. Therefore model accuracy and sensitivity is requested particularly in the most critical operating conditions corresponding to medium-high load, rather than at low load. In such conditions, the model exhibits a mean validation error below 23%, which is comparable to the accuracy achieved by physical models, even more complex that this, presented in the literature (Jung and Assanis, 2006; Patterson *et al.*, 1994; Hountalas, 2008; Miller *et al.*, 1998).

3 COMBUSTION NOISE

Noise is a critical issue for automotive engines and its main source is the in-cylinder pressure gradient generated during combustion. The in-cylinder pressure acts as exciting force on the engine block, causing its vibration and finally resulting in radiated noise (Payri *et al.*, 2005). The combustion noise generated by the sharp increase of in-cylinder pressure is strongly affected by the heat release rate (*i.e.* fuel burning rate) which in turn

depends on injection pattern and mixture composition (*i.e.* air, fuel and inert gases). The presented methodology is aimed at predicting the impact of these control variables on combustion noise.

Mechanical noise, generated by the mechanical forces related to moving components (*i.e.* camshafts, connecting rods, pistons, etc.), also concurs to block vibration and noise radiation. Nevertheless it is not affected by engine control and its analysis was neglected, being beyond the scope of the present work.

The proposed approach is based on the estimation of the Sound Pressure Level (SPL), defined as:

$$SPL = 20 \times \log_{10}\left(\frac{p_{eff}}{p_0}\right) \tag{22}$$

The reference value p_0 corresponds to the hearing threshold at a frequency of 1 kHz and is set to 2×10^{-5} Pa. The sound pressure p_{eff} represents the root mean square of the time domain pressure signal and is given by:

$$p_{eff} = \sqrt{\frac{1}{T_{eff}}\int_0^T p(t)^2 dt} \tag{23}$$

Equation (22) is supposed to be applied for pure tones. In case of complex signals, as it is the case for the in-cylinder pressure, decomposition in elementary harmonics has to be accomplished by means of FFT analysis.

The methodology was applied to the simulated in-cylinder pressure traces corresponding to the test cases 1, 3, and 4 previously considered for model validation (*Tab. 3*). This allows analyzing engine working conditions with different speed, load and EGR rate. SPL estimation was performed considering the in-cylinder pressure contribution of all cylinders, as it is shown in Figure 15, to better describe the excitation of the engine structure. The resulting SPL frequency spectra are shown in Figure 16. As expected, the test cases with higher speed and load show a greater SPL in almost the whole frequency band. The maximum values are located at the lowest frequencies corresponding to the combustion period and are dependent on the magnitude of the in-cylinder pressure peak. On the other hand, at medium frequencies (*i.e.* 1 KHz), the SPL of the three test cases almost superimpose due to the impact of the higher pressure gradient following the enhanced premixed combustion for earlier injections and greater EGR rate.

In order to indicate the overall noise generated by the in-cylinder pressure signal, a synthetic index is introduced by the following equation, corresponding to the law of level summation (Möser, 2009):

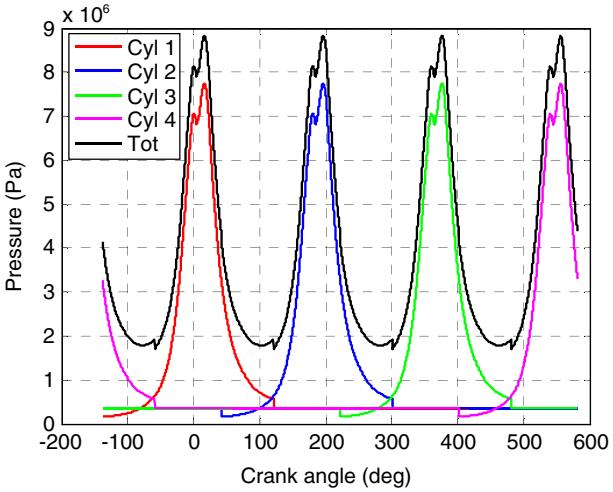

Figure 15

Superposition of the in-cylinder pressure in the four cylinders for the test case 1. The abscissa window corresponds to one engine cycle.

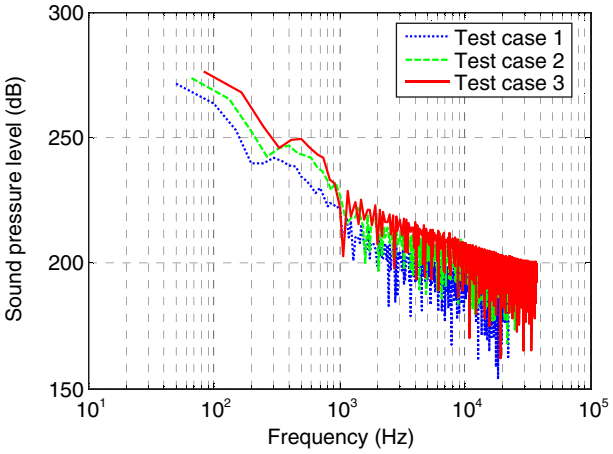

Figure 16

Frequency spectra of SPL for the three considered working conditions.

$$SPL_{tot} = 10 \times \log_{10} \sum_{i=1}^{N} 10^{\frac{SPL_i}{10}} \tag{24}$$

This approach allows estimating the total (or global) sound pressure level in case of more noise sources, as it is the case of the complex in-cylinder pressure signal that exhibits different harmonic components.

Figure 17 shows the estimation of the total SPL for the three working conditions considered. As expected from the SPL spectra analysis shown in Figure 16, the total SPL increases with load as it is mostly influenced

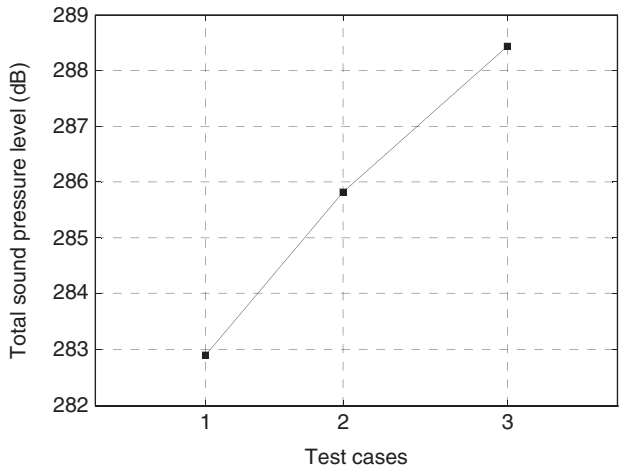

Figure 17

Total SPL for the three test cases considered for model validation.

by the greatest values at low frequencies which are related to in-cylinder peak pressure magnitude.

4 RESULTS AND DISCUSSION

The present section analyzes the impact of combustion control variables, namely fuel injection pattern and EGR rate, on heat release rate, in-cylinder pressure and, consequently, noise and pollutants emissions of NO and soot. The analysis is based on the multi-zone model simulations coupled with the methodology for combustion noise prediction. Simulations were carried out at fixed engine speed (*i.e.* 2 000 rpm) and overall amount of injected fuel (*i.e.* 20 mg/cycle), imposing variation of EGR rate, rail pressure and Start of Injection (SOI), as reported in Table 4. A multiple injection strategy with pilot, pre and main injections was applied in all cases.

4.1 Start of Injection

The impact of SOI was investigated by imposing a variation from the baseline values, set to −30/−16/−3°ATDC (for pilot, pre and main injections, respectively), towards BDC up to −60° ATDC for the pilot injection. Fuel delivered for each injection and dwell times were kept constant, consequently as pilot SOI was advanced, pre and main injection were shifted accordingly.

Figures 18 and 19 show the superposition of pressure cycles and heat release rate profiles simulated at fixed

TABLE 4

Set-points of the combustion control variables investigated to analyze the impact on performance and emissions

P_{rail} (bar)	EGR (%)	SOI (°ATDC)
700	20	Pilot from −30 to −60 by steps of −10
	30	Pre from −16 to −46 by steps of −10
	40	Main from −3 to −33 by steps of −10
1 000	30	Pilot from −30 to −60 by steps of −10
		Pre from −16 to −46 by steps of −10
		Main from −3 to −33 by steps of −10

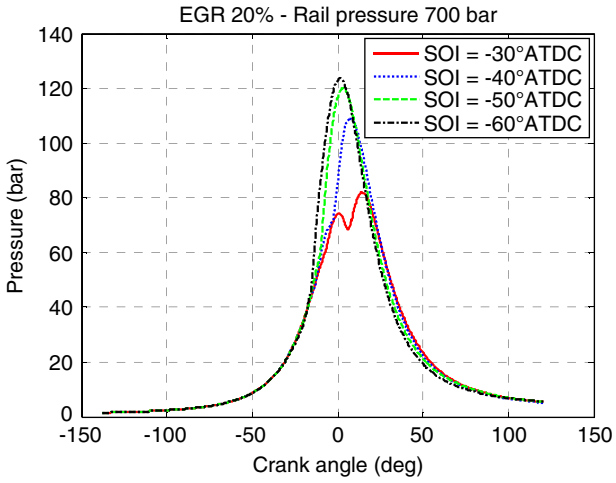

Figure 18

Simulated in-cylinder pressure at different pilot SOI and fixed EGR and rail pressure.

EGR and rail pressure and variable SOI. According to Figure 18, as the SOI is advanced the in-cylinder pressure exhibits a significant increase. This behavior is explained by the heat release rate profiles shown in Figure 19. As the SOI is advanced, the ignition delay is increased, due to the lower in-cylinder temperature (*Eq. 11*), particularly for the pilot and pre injections. The figure evidences that when SOI advance is greater than 40° the heat release of pilot, pre and main injection take place simultaneously, reducing the benefits of multiple injection. As a consequence of the increased ignition delay, the in-cylinder pressure exhibits a greater pressure rise due to the enhanced air-fuel mixing and the larger fraction of fuel burning in premixed mode.

It is worth noting that further advancing SOI towards BDC would amplify these phenomena, promoting a

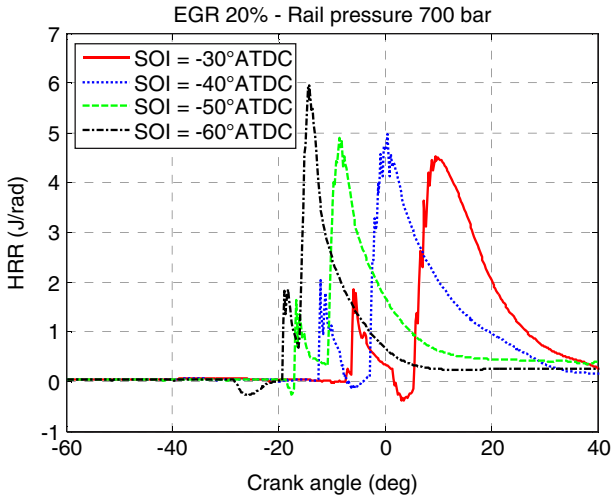

Figure 19

Simulated heat release rate at different pilot SOI and fixed EGR and rail pressure.

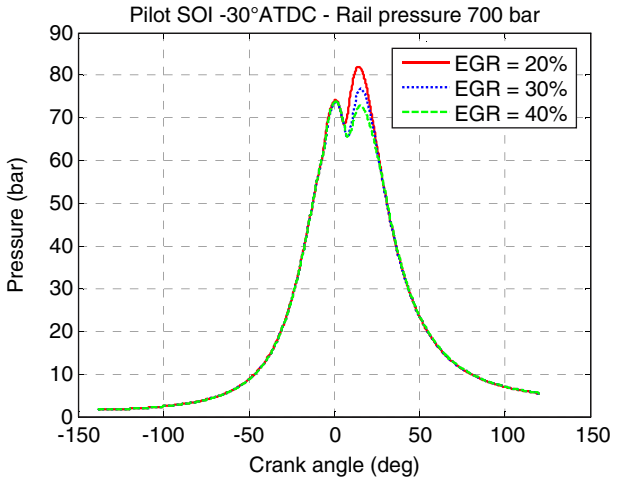

Figure 20

Simulated in-cylinder pressure at different EGR rates and fixed SOI and rail pressure.

complete premixed combustion (*i.e.* Premixed Combustion Compression Ignition – PCCI) in place of the conventional one. Nevertheless, though innovative combustion concepts, such as PCCI, have experimentally proved to be promising in reducing both NO and soot emissions, they were not investigated in the current analyses. The motivation is that advancing injection may result in combustion deterioration and fuel impingement on cylinder or piston walls and none of these effects is actually taken into account by the in-cylinder model.

4.2 Exhaust Gas Recirculation

The impact of inert gases and oxygen concentration in the intake charge was analyzed by considering three EGR rates, corresponding to 20% (*i.e.* baseline setting), 30% and 40%. Figure 20 exhibits that as EGR is increased the in-cylinder pressure presents a lower peak and smoother rise. According to Figure 21 this is due to the less abrupt combustion, due to the lower temperature and oxygen content in the mixing zone (*Eq. 16*).

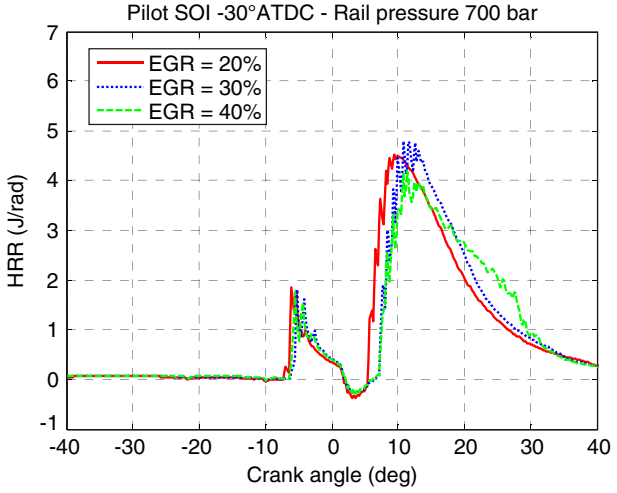

Figure 21

Simulated heat release rate at different EGR rates and fixed SOI and rail pressure.

4.3 Rail Pressure

Two values of injection pressure were considered for the present analysis, corresponding to 700 bar (*i.e.* baseline setting) and 1 000 bar. The increase of injection pressure results in better fuel atomization and improved air-fuel mixing due to the greater flux momentum. The resulting in-cylinder pressure exhibits a greater rise following the enhanced air-fuel mixing. This is evidenced by Figures 22 and 23 that show in-cylinder pressure and heat release rate for the two considered values of injection pressure with fixed SOI and EGR.

4.4 Engine Performance and Emissions

The impact of combustion control variables on engine performance and emissions is shown in the following

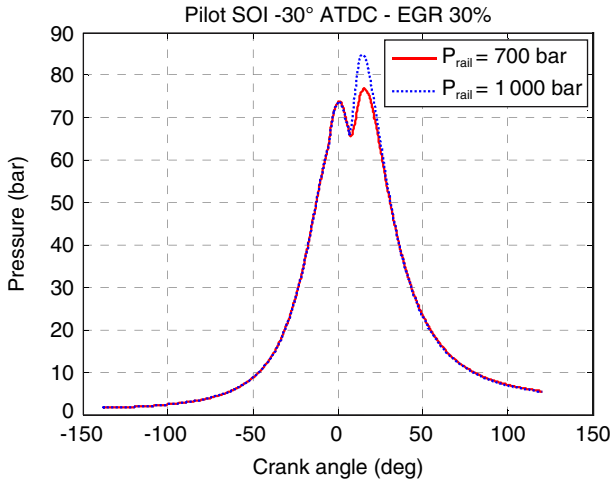

Figure 22

Simulated in-cylinder pressure at different rail pressure and fixed SOI and EGR rate.

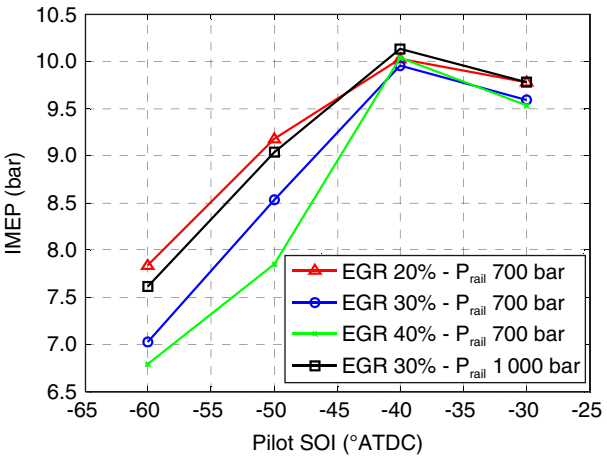

Figure 24

Simulation results: effect of SOI, EGR and P_{rail} on IMEP.

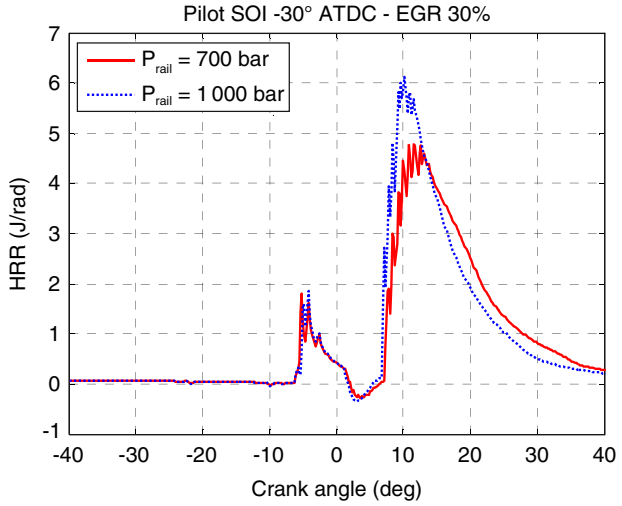

Figure 23

Simulated heat release rate at different rail pressure and fixed SOI and EGR rate.

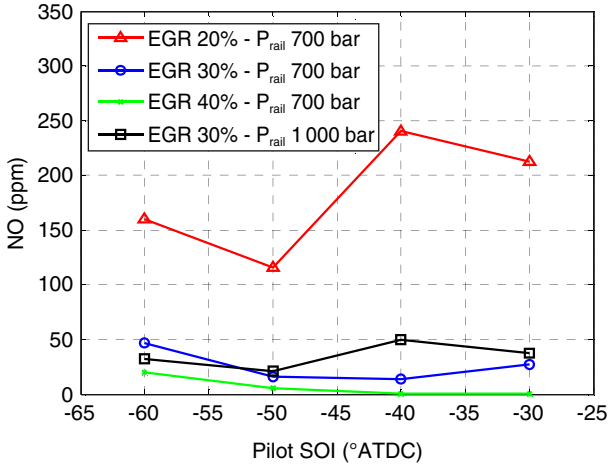

Figure 25

Simulation results: effect of SOI, EGR and P_{rail} on NO emissions.

Figures 24-27 that illustrate the prediction of IMEP, NO, soot and combustion noise in the operated conditions investigated (*Tab. 4*).

Figure 24 shows that as SOI is advanced the IMEP initially increases due to in-cylinder pressure rise, until pilot SOI reaches approx. −40°. As SOI is further advanced towards TDC, IMEP decreases due to the higher compression work. The opposite impact of EGR and rail pressure on IMEP reflects the behavior of pressure cycle and heat release rate, previously commented in Figures 20-23. It is worth noting that following the assumption of constant mass of injected fuel per cycle, an increase of IMEP corresponds to higher combustion efficiency, with lower specific fuel consumption and CO_2 emissions.

Figure 25 shows that as SOI is advanced, NO emissions initially increase for the higher in-cylinder temperature following the sharp heat release rate (*Fig. 19*). Further SOI advance results in a reduction of NO due to more uniform air-fuel mixing and reduced local

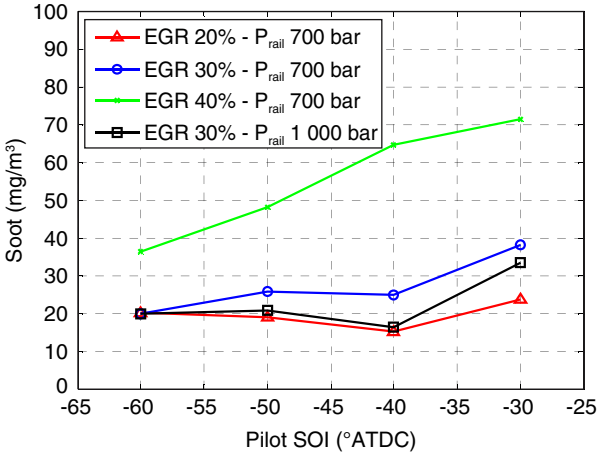

Figure 26

Simulation results: effect of SOI, EGR and P_{rail} on soot emissions.

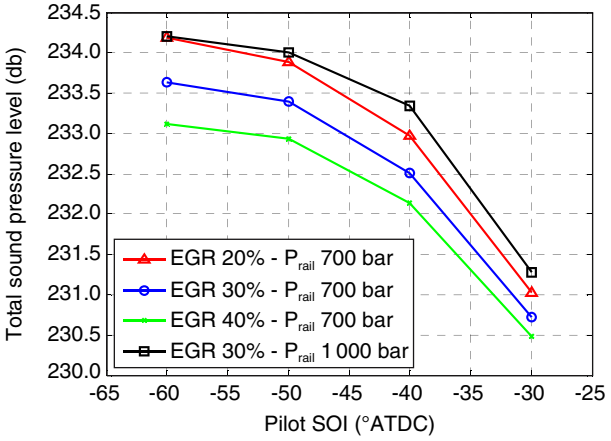

Figure 27

Simulation results: effect of SOI, EGR and P_{rail} on combustion noise.

temperature. Both these effects are enhanced by the rail pressure, due to the mentioned influence on fuel atomization and air-fuel mixing. Concerning the EGR rate, Figure 25 exhibits the expected strong impact on NO reduction, due to the significant temperature decrease.

The prediction of soot emissions confirms the expected trade-off with NO emissions. Figure 26 shows that as SOI is advanced soot emissions decrease due to the enhanced air-fuel mixing caused by the longer ignition delay. This phenomenon is even amplified by the higher rail pressure that promotes fuel atomization and air entrainment. On the other hand, high EGR rate results in an increase of soot due to the lower temperature that inhibits soot oxidation.

The impact on combustion noise is shown in Figure 27 and reflects the heat release rate profiles (*Fig. 19, 21, 23*). Advanced SOI and high injection pressure promote premixed combustion, resulting in a sharp heat release rate and a greater sound pressure level. This effect is mitigated by the low oxygen concentration in case of high EGR that makes combustion rate smoother.

In order to highlight the opposite effects of combustion control variables on engine performances and emissions, Figures 28 and 29 show the simulated trade-off of IMEP *versus* SPL and NO *versus* soot emissions, respectively. The simulations were performed imposing constant engine speed (*i.e.* 2 000 rpm), mass of injected fuel (*i.e.* 20 mg/cycle) and SOI (−30°/−16°/−3°ATDC) while ranging EGR rate and rail pressure as reported in Table 5.

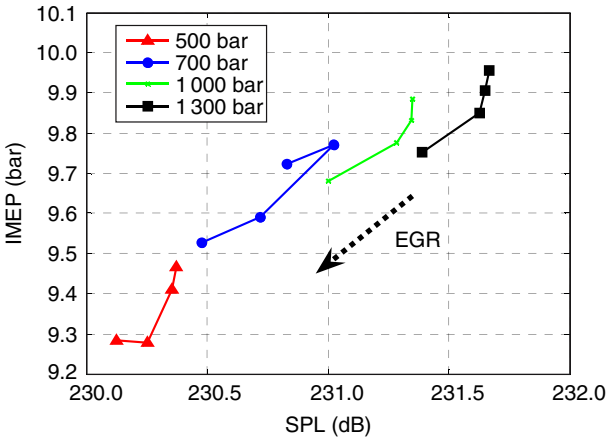

Figure 28

Simulation results: trade-off between acoustic emissions (SPL) and Indicated Mean Effective Pressure (IMEP).

Particularly, the figures evidence that increasing the rail pressures results in higher IMEP (*i.e.* lower specific fuel consumption) and lower soot emissions with a slight impact on NO emissions. Nevertheless a strong increase of combustion noise is observed. On the other hand, increasing the EGR rate results in a strong reduction of both NO and noise and an increase of specific fuel consumption (*i.e.* reduction of IMEP) and soot.

The presented results evidence that the quasi-dimensional multi-zone modeling approach applied for in-cylinder simulation allows predicting the expected trends of pressure cycle and heat release rate *versus*

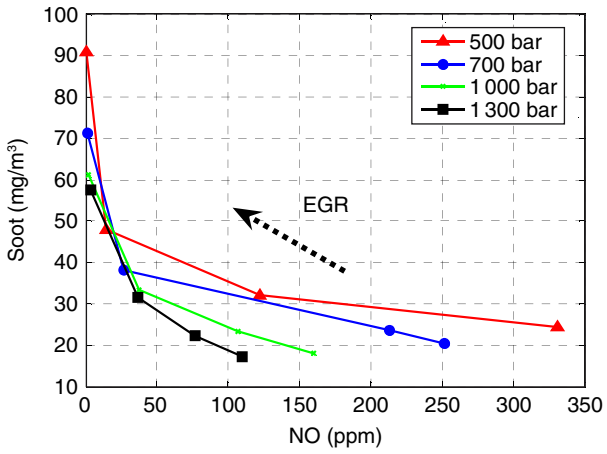

Figure 29

Simulation results: trade-off between soot and NO emissions.

TABLE 5

Operating conditions investigated for the trade-off analysis

P_{rail} (bar)	500 / 700 /1 000 / 1 300
EGR (%)	10 / 20 / 30 / 40

injection pattern and EGR rate. Consequently the effects on engine performance, noise and pollutants are in accordance with those expected from the experimental analyses in the literature (Tennison and Reitz, 2001; Torregrosa *et al.*, 2011). Particularly, the simulation results confirm the complex interaction and the opposite effects of injection timing, injection pressure and EGR on fuel burning rate and pollutants formation and evidence the valuable contribution of simulation models for EMS tuning.

CONCLUSIONS

The impact of injection pattern and EGR on noise and pollutants emissions in a light-duty Diesel engine was investigated *via* simulation analysis. A Multi-zone quasi dimensional model was applied for combustion simulation and NO/soot estimation and successfully validated against experimental data. Furthermore a methodology based on in-cylinder pressure processing was applied for combustion noise prediction.

The simulated effects of injection timing, rail pressure and EGR on engine performance, noise and pollutants were in accordance with those expected from the experimental analyses proposed in the literature. Particularly, the simulation results confirmed the complex interaction and the opposite effects on fuel burning rate and pollutants formation and evidenced the valuable contribution of the proposed modeling approach for EMS tuning.

Future work will be aimed at improving the fuel jet model to account for combustion deterioration and fuel wall impingement which usually take place in case of advanced injection timing characteristic of premixed combustion (*i.e.* PCCI).

ACKNOWLEDGMENTS

The present research has been funded by Magneti Marelli S.p.A. Powertrain and University of Salerno.

REFERENCES

Arsie I., Pianese C., Rizzo G. (1998) Models for the Prediction of Performance and Emissions in a Spark Ignition Engine - A Sequentially Structured Approach, *SAE Technical Paper* 980779.

Arsie I., Di Genova F., Mogavero A., Pianese C., Rizzo G., Caraceni A., Cioffi P., Flauti G. (2006) Multi-Zone Predictive Modeling of Common-Rail Multi-Injection Diesel Engines, *SAE Technical Paper* 2006-01-1384.

Arsie I., Pianese C., Sorrentino M. (2007) Effects of Control Parameters on Performance and Emissions of HSDI Diesel Engines: Investigation *via* Two Zone Modelling, *Oil & Gas Science and Technology* **62**, 4, 457-469.

Arsie I., Di Leo R., Pianese C., De Cesare M. (2012) Combustion Noise and Pollutants Prediction for Injection Pattern and EGR Tuning in an Automotive Common-Rail Diesel Engine, *IFAC Workshop on Engine and Powertrain Control, Simulation and Modeling (E-COSM'12)*, Rueil-Malmaison (France), 23-25 Oct.

Assanis D.N., Heywood J.B. (1986) Development and Use of a Computer Simulation of the Turbocompounded Diesel System for Engine Performance and Component Heat Transfer Studies, *SAE Technical Paper* 860329.

Ayoub N.S., Reitz R. (1995) Multidimensional Computation of Multicomponent Spray Vaporization and Combustion, *SAE Technical Paper* 950285.

Barba C., Burkhardt C., Boulouchos K., Bargende M. (2000) A Phenomenological Combustion Model for Heat Release Rate Prediction in High-Speed DI Diesel Engines With Common Rail Injection, *SAE Technical Paper* 2000-01-2933.

Bayer J., Foster D.E. (2003) Zero-Dimensional Soot Modeling, *SAE Technical Paper* 2003-01-1070.

Bi X., Yang M., Han S., Ma Z. (1999) A Multi-Zone Model for Diesel Spray Combustion, *SAE Technical Paper* 1999-01-0916.

Coppo M., Dongiovanni C. (2007) Experimental Validation of a Common-Rail Injector Model in the Whole Operation Field, *ASME J. of Engineering for Gas Turbines and Power* **129**, 596-608.

Ferguson C.R. (1986) Internal Combustion Engine, *Applied Thermosciences*, John Wiley.

Gang L., Tao B. (2010) Multiple-Cylinder Diesel Engine Combustion CFD Simulation with Detailed Chemistry Based IPV-Library Approach, *SAE Technical Paper* 2010-01-1495.

Heywood J.B. (1988) *Internal Combustion Engine Fundamentals*, MC Graw Hill.

Hiroyasu H., Masataka A. (1990) Structures of Spray in Diesel Engines, *SAE Technical Paper* 900475.

Hiroyasu H., Kadota T. (1983) Development and Use of a Spray Combustion Modeling to Predict Diesel Engine Efficiency and Pollutant Emission, *Bulletin of the ASME* **26**, 214.

Hountalas D.T., Mavrapoulos G.C., Binder K.B. (2008) Effect of Exhaust Gas Recirculation (EGR) temperature for various EGR rates on heavy duty DI Diesel engine performance and emissions, *Energy* **33**, 272-283.

Javadi Rad G., Gorjiinst M., Keshavarz M., Safari H., Jazayeri A.A. (2010) An Investigation on Injection Characteristics of Direct-Injected Heavy Duty Diesel Engine by Means of Multi-Zone Spray Modeling, *Oil & Gas Science and Technology* **65**, 893-901.

Jung D., Assanis D.N. (2006) Quasidimensional Modeling of Direct Injection Diesel Engine Nitric Oxide, Soot, and Unburned Hydrocarbon Emissions, *ASME J. of Engineering for Gas Turbines and Power* **128**, 388-396.

Kong S.C., Han Z., Reitz R.D. (1995) The Development and Application of a Diesel Ignition and Combustion Model for Multidimensional Engine Simulation, *SAE Technical Paper* 950278.

Kouremenos D.A., Rakopoulos C.D., Hountalas D.T. (1997) Multi-Zone Combustion Modeling for the Prediction of Pollutant Emissions and Performance of DI Diesel Engine, *SAE Technical Paper* 970635.

Kuo K.K. (1986) *Principles of Combustion*, John Wiley.

López J.J., Novella R., García A., Winklinger J.F. (2013) Investigation of the ignition and combustion processes of a dual-fuel spray under Diesel-like conditions using Computational Fluid Dynamics (CFD) modelling, *Mathematical and Computer Modeling* **57**, 1897-1906.

Miller R., Davis G., Lavoie G., Newman C., Gardner T. (1998) A Super-Extended Zel'dovich Mechanism for NO_x Modeling and Engine Calibration, *SAE Technical Paper* 980781.

Möser M. (2009) *Engineering acoustics – An introduction to Noise Control*, Springer.

Naber J.D., Siebers D.L. (1996) Effects of gas Density and Vaporization on Penetration and Dispersion of Diesel Spray, *SAE Technical Paper* 960034.

Patterson M.A., Kong S.C., Hampson G.J., Reitz R.D. (1994) Modeling the Effects of Fuel Injection Characteristics on Diesel Engine Soot and NO_x Emissions, *SAE Technical Paper* 940523.

Payri F., Broatch A., Tormos B., Marant V. (2005) New methodology for in-cylinder pressure analysis in direct injection Diesel engines – Application to combustion noise, *Meas. Sci. Technol.* **16**, 540-547.

Rakopoulos C.D., Rakopoulos D.C., Kyritsis D.C. (2003) Development and Validation of a Comprehensive two-zone Model for Combustion and Emissions Formation in a DI Diesel Engine, *International Journal of Energy Research* **27**, 1221-1249.

Ramos J.I. (1989) *Internal Combustion Engine Modeling*, Hemisphere Publishing Corporation.

Tanner F.X., Reitz R.D. (1999) Scaling Aspects of the Characteristic Time Combustion Model in the Simulation of Diesel Engines, *SAE Technical Paper* 1999-01-1175.

Tennison P.J., Reitz R.D. (2001) An Experimental Investigation of the Effects of Common-Rail Injection System Parameters on Emissions and Performance in a High-Speed Direct-Injection Diesel Engine, *ASME J. of Engineering for Gas Turbines and Power* **123**, 167-178.

Torregrosa A.J., Broatch A., Novella R., Mónico L.F. (2011) Suitability analysis of advanced Diesel combustion concepts for emissions and noise control, *Energy* **36**, 825-838.

Manuscript accepted in November 2013
Published online in April 2014

Cite this article as: I. Arsie, R. Di Leo, C. Pianese and M. De Cesare (2015). Combustion Noise and Pollutants Prediction for Injection Pattern and Exhaust Gas Recirculation Tuning in an Automotive Common-Rail Diesel Engine, *Oil Gas Sci. Technol* **70**, 1, 91-109.